Order online now!

www.rockland.com
tech@rockland.com
+1 484.791.3823

Datasheet for 600-401-880

Alpha-Tubulin Antibody

Overview

Description:	Anti-Alpha-Tubulin (RABBIT) Antibody - 600-401-880
Item No.:	600-401-880
Size:	200 µg
Applications:	ELISA, IF, WB, IP, Other
Reactivity:	Human, Mouse, Rat
Host Species:	Rabbit

Product Details

Background:	Tubulin Loading Control Antibody recognizes microtubules which are involved in a wide variety of cellular activities ranging from mitosis and transport events to cell movement and the maintenance of cell shape. Tubulin itself is a globular protein consisting of two polypeptides (alpha and beta tubulin). Alpha and beta tubulin dimers are assembled to 13 protofilaments that form a microtubule of 22-nm diameter. Tyrosine ligase adds a C-terminal tyrosine to monomeric alpha tubulin. Assembled microtubules can again be detyrosinated by a cytoskeleton-associated carboxypeptidase. Detyrosinated alpha tubulin is referred to as Glu-tubulin. Another post-translational modification of detyrosinated alpha tubulin is C-terminal polyglutamylation, which is characteristic of microtubules in neuronal cells and the mitotic spindle. This antibody makes an excellent loading control. Anti-Alpha-tubulin antibody is ideal for investigators involved in cell cycle protein research.
Synonyms:	rabbit anti-alpha-Tubulin Antibody, rabbit anti-α-tubulin antibody, Tubulin alpha-1B chain, Tubulin alpha-ubiquitous chain, Alpha-tubulin ubiquitous, Tubulin K-alpha-1, TUBA1B, tubulin loading control, Alpha-tubulin, Tubulin alpha-1A, TUBA1A, TUBA3, LIS3
Host Species:	Rabbit
Clonality:	Polyclonal
Format:	IgG

Target Details

Gene Name:	TUBA1B
Reactivity:	Human, Mouse, Rat

Immunogen Type:	Conjugated Peptide
Immunogen:	Anti-Tubulin Loading Control Antibody was prepared from whole rabbit serum produced by repeated immunizations with a synthetic peptide corresponding to the C-Terminal region near amino acids 425-451 of Human alpha Tubulin.
Purity/Specificity:	Anti-Tubulin Loading Control Antibody is directed against human alpha Tubulin protein. The Loading Control Antibody was affinity purified from monospecific antiserum by immunoaffinity purification. A BLAST analysis was used to suggest that this antibody would react with alpha Tubulin from a wide range of organisms, including avian, mammalian aquatic, parasitic and alga sources based on 100% homology for the immunogen sequence. Cross reactivity will occur with all isoforms of alpha tubulin. Such broad reactivity makes this antibody useful as an excellent loading control.
Relevant Links:	• NCBI - 17986283 • UniProtKB - P68363

Application Details

Tested Applications:	ELISA, IF, WB
Suggested Applications:	IP, Other (Based on references)
Application Note:	Anti-Tubulin Antibody has been tested for use in ELISA, immunofluorescence, and western blot. Specific conditions for reactivity should be optimized by the end user. Expect a band at ~50 kDa in size corresponding to alpha tubulin by western blotting in most cell lysates or extracts.
Assay Dilutions:	All assays should be optimized by the user. Recommended dilutions (if any) may be listed below.
ELISA:	1:90,000
IF:	1:500 - 1:2,000
IHC:	1:500 - 1:2,000
WB:	1:1,000 - 1:5,000

Formulation

Physical State:	Liquid (sterile filtered)
Concentration:	1.1mg/ml by UV absorbance at 280 nm
Buffer:	0.02 M Potassium Phosphate, 0.15 M Sodium Chloride, pH 7.2
Preservative:	0.01% (w/v) Sodium Azide
Stabilizer:	None

Shipping & Handling

Shipping Condition:	Dry Ice
Storage Condition:	Store Anti-Tubulin Loading Control Antibody at -20° C prior to opening. Aliquot Loading Control Antibody contents and freeze at -20° C or below for extended storage. Avoid cycles of freezing and thawing. Centrifuge Tubulin Loading Control Antibody if not completely clear after standing at room temperature. This Control Antibody is stable for several weeks at 4° C as an undiluted liquid. Dilute only prior to immediate use.
Expiration:	Expiration date is one (1) year from date of receipt.

Images

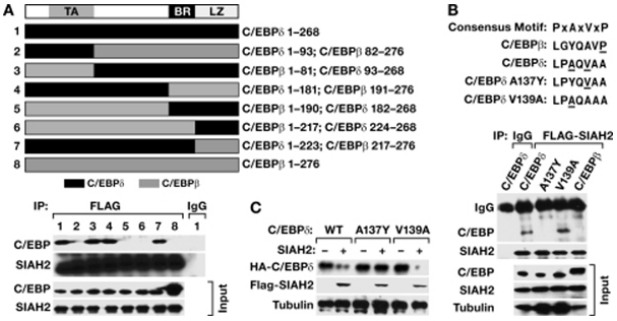

Western Blot
Identification of the SIAH2 interaction domain in C/EBPδ. (A) Six different C/EBPδ-C/EBPβ chimeric proteins, as shown in the schematic and the full-length proteins, were cotransfected with Flag-SIAH2 in MCF-10A cells. Immunoprecipitates with anti-Flag antibody and input were analyzed with a pan-C/EBP and anti-Flag antibody for SIAH2. Cells had been treated with MG132 to stabilize C/EBPδ. TA, transactivation domain; BR, basic region; LZ, leucine zipper. (B) Schematic of the sequence of human C/EBPδ and C/EBPβ aligned with the consensus for SIAH2 interaction domains and two point mutations in C/EBPδ (underlined amino acids match the consensus motif). Immunoprecipitates with anti-Flag antibody and input were analyzed with antibodies specific for C/EBPβ and C/EBPδ and with anti-Flag to detect SIAH2. Cells had been treated with MG132 to stabilize C/EBPδ. (C) Western analysis of MCF-10A cells after transfection with the indicated C/EBPδ expression constructs and Flag-SIAH2. Fig 5. PMID: 22037769

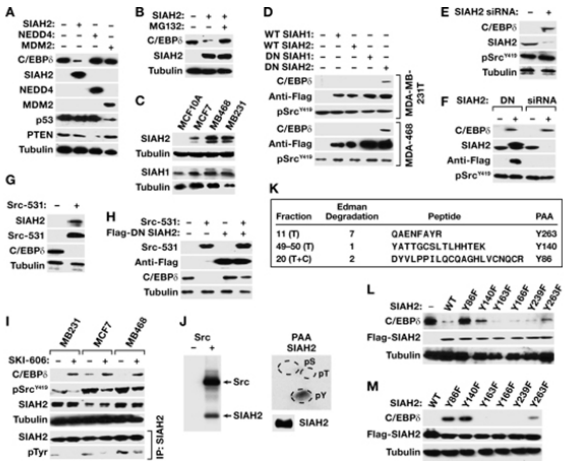

Western Blot

SIAH2 is necessary and sufficient for C/EBPδ downregulation. (A) Western analysis of MCF-10A cells transfected with expression constructs for the indicated proteins. (B) MCF-10A cells were transfected with SIAH2, treated with MG132, and analyzed as described in panel A. (C) Western analysis of the indicated cell lines for SIAH1 and SIAH2 expression. (D) Western analysis of MDA-MB-231T (top) and MDA-MB-468 (bottom) cells transfected with the indicated SIAH proteins, which were detected with anti-Flag antibodies. (E) Western analysis of MDA-MB-231T cells after nucleofection of siRNA against SIAH2. (F) Western analysis of MDA-MB-231T cells transfected with a DN-SIAH2 expression construct or nucleofected with siRNA against SIAH2. Anti-Flag was used to detect specifically DN-SIAH2, which has a higher MW than endogenous SIAH2. (G) Western analysis of MCF-10A cells transfected with Src-531. (H) Western analysis of MCF-10A cells cotransfected with Src-531 and/or DN-SIAH2. (I) Western analysis of the indicated cell lines treated with SKI-606 for 24 h. The same lysates were immunoprecipitated with anti-SIAH2 and immunoblotted with anti-phospho-tyrosine. (J) In vitro phosphorylation assay conducted by incubating affinity purified Flag-SIAH2 with (+) or without (−) purified Src-530 in the presence of [32P]ATP. Samples were resolved by SDS-PAGE, transferred to nitrocellulose, and subjected to autoradiography (left panel). Labeled SIAH2 was digested from the membrane and subjected to phosphoamino acid analysis (PAA; right panel). Expression of the input SIAH2 by Western analysis is also shown. (K) Results from HPLC analysis of SIAH2 with or without individual tyrosine-to-phenylalanine mutations (see panel L) after in vitro phosphorylation assays as in panel J, compared to unphosphorylated WT SIAH2, Edman degradation, and phosphoamino acid analysis. T, trypsin; T +C; trypsin followed by chymotrypsin. (L) Western analysis of MCF-10A cells transfected with expression constructs for the indicated SIAH2 proteins. (M) Western analysis of MDA-MB-231 cells transfected as described for panel L.
Fig 3. PMID: 22037769

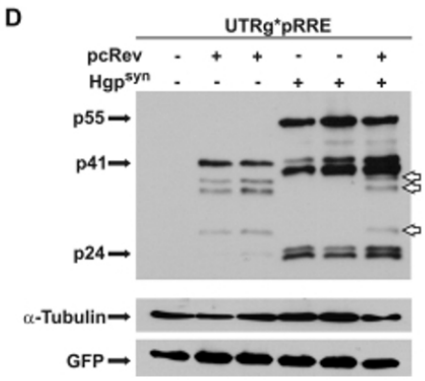

Western Blot
(D) Western blot analysis with an anti-p24CA antibody detected the wild-type Gag protein pattern from the codon-optimized Hgpsyn and truncated Gag isoforms (white arrows) encoded by UTRg*pRRE. Shown are results of two independent cotransfections with pcRev (lanes 2 and 3) and Hgpsyn (lanes 4 and 5). Loading of similar amounts of protein was verified by incubation of the stripped Western blot with an antibody against the endogenous protein α-tubulin. Transfection efficiencies were similar, as demonstrated by a separate Western blot analysis against GFP encoded by the cotransfected pEGFP-C1. Fig 3.
PMID: 22258250

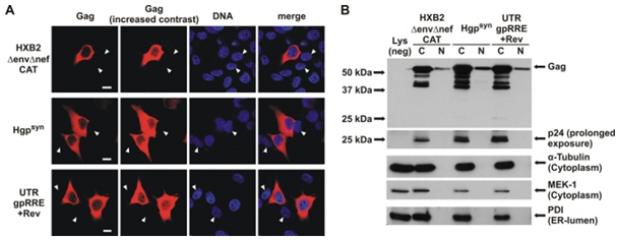

Western Blot
Detection of nucleus-localized Gag. (A) HeLa cells transfected with the indicated gag/gag-pol expression plasmids were analyzed by confocal immunofluorescence microscopy. To demonstrate nuclear Gag signals, the contrast of anti-Gag immunofluorescence images was increased postimaging (Adobe Photoshop). White arrowheads mark examples of nuclei of untransfected cells that do not show nuclear Gag fluorescence after a contrast increase. White scale bars represent 10 µm. (B) Transfected HEK 293T cells were fractionated into nuclear (N) and cytoplasmic (C) fractions for anti-p24CA Western blot analysis. The stripped blot was incubated with an antibody against the cytoplasmic protein α-tubulin. Furthermore, the purity of the nuclear fractions was demonstrated by the lack of different cytoplasmic marker proteins. Fig 6.
PMID: 22258250

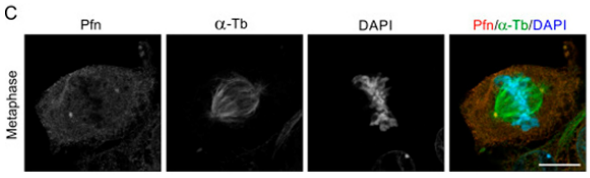

Immunofluorescence Microscopy
(C) High-resolution confocal microscopy (AiryScan) of a metaphase cell after simultaneous staining for Pfn, α-tubulin (α-Tb), and DNA (DAPI). Scale bars 10 µm. SF1.
PMID: 33184056

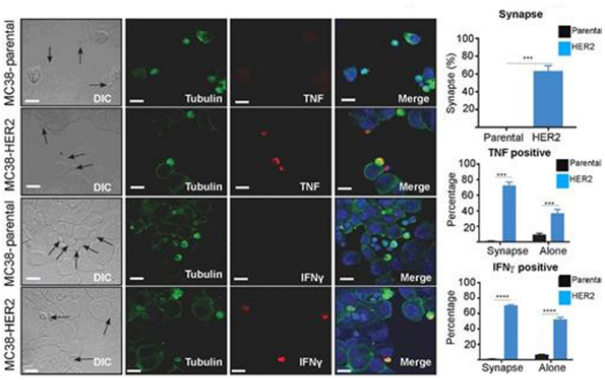

Immunofluorescence Microscopy
C, Left, MC38-HER2 or parental cells were seeded in chamber slides, then overlaid with CAR T cells. After 2 hours, cells were fixed and stained as indicated, then visualized by confocal microscopy. Scale bar, 10 µm. Right, the percentage of CAR T cells that formed an immunologic synapse was quantitated by confocal microscopy (>100 cells). The percentage of CAR T cells positive for the indicated cytokines was quantitated by confocal microscopy (>100 cells). Fig 1. PMID: 30651288

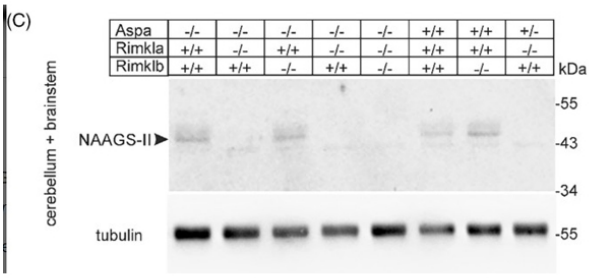

Western Blot
(C) Western blot analysis of the Rimkla encoded NAAGS-II in homogenates from cerebellum and brainstem isolated from 7-month-old mice of the indicated genotypes confirmed absence of NAAGS-II in Rimkla deficient mice. Blots were reprobed with anti-tubulin antibody for loading control. Fig 2. PMID: 38011891

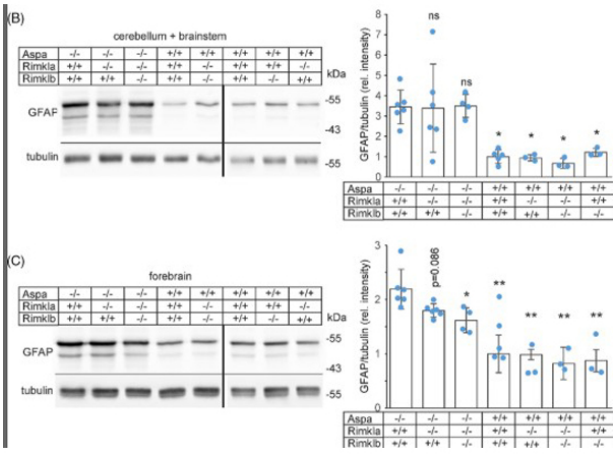

Western Blot
(B) Western blot analysis of GFAP in cerebellum with brainstem and densitometric quantification (normalized to tubulin) (n = 3–6). (C) Western blot analysis of GFAP in forebrain samples and densitometric quantification (normalized to tubulin) (n = 3–6). Densitometric quantification indicated astrogliosis in all Aspanur7/nur7 (Aspa−/−) mice irrespective of their Rimkla and Rimklb genotype. GFAP level was significantly reduced in the forebrain of Aspa+/+/Rimkla−/−/Rimklb−/− mice. *p < 0.05, **p < 0.001; and ns, not significant. Fig 5. PMID: 38011891

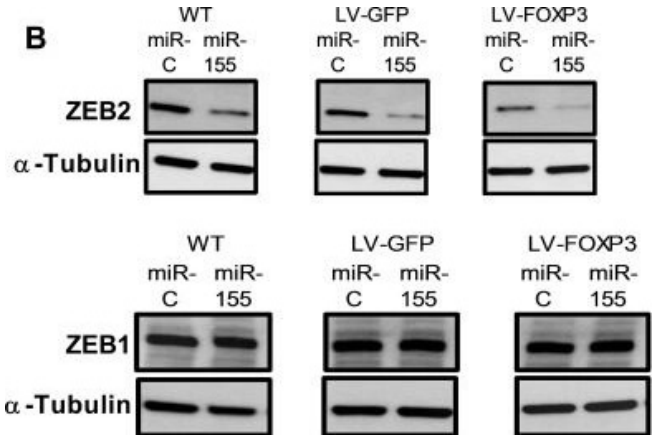

Western Blot
miR-155 and FOXP3 down regulate endogenous ZEB2 in human breast cancer cells resulting in altered levels of EMT markers Vimentin and E-cadherin(A) Relative abundance of ZEB2 and ZEB1 protein in WT, GFP or FOXP3 overexpressing BT549 cells transfected with miR-155 or miR-control. Relative abundance of protein was determined by quantitation of the abundance of ZEB2 or ZEB1 proteins normalised to reference protein α-Tubulin by western blot analysis. Quantitation of bands was carried out using Image J software. Mean + SD plotted. Student's t test ***P < 0.001. ZEB1 protein expression as above. n = 3 experiments. (B) ZEB2 and ZEB1 protein in WT, GFP or FOXP3 overexpressing BT549 cells transfected with miR-155 or miR-control by western blot. Representative western blot shown. (C) Relative abundance of Vimentin and E-cadherin protein in WT, GFP or FOXP3 overexpressing BT549 cells transfected with miR-155 or miR-control. Relative abundance of protein was determined by quantitating the abundance of E-cadherin or Vimentin proteins and normalising to reference protein β-Actin by western blot analysis. Quantitation of bands was carried out using Image J software. Mean + SD plotted. Student's t test ***P < 0.001, **P < 0.01. n = 3 experiments. (D) Vimentin and E-cadherin protein in WT, GFP or FOXP3 overexpressing BT549 cells transfected with miR-155 or miR-control analysed by western blot. Representative western blot shown. Figure provided by CiteAb. Source: Oncotarget, PMID: 29963231.

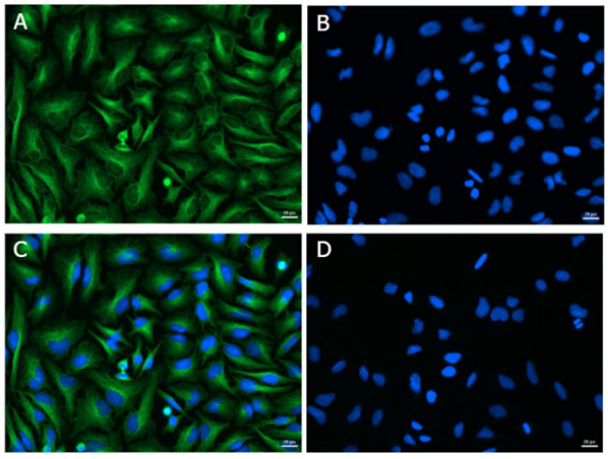

Immunofluorescence Microscopy
Immunofluorescence of Rabbit Anti-Alpha Tubulin Antibody.
Cell line: HeLa.
Primary Antibody: Alpha Tubulin (p/n 600-401-880) at 4.4 µg/mL (1:250) for 1hr at RT.
Secondary Antibody: Goat Anti-Rabbit DyLight™ 488 (p/n 611-141-121) at 1 µg/mL (1:1000) overnight at 4 °C.
Fixative: Ice Cold Methanol.
Permeabilization: Ice Cold Methanol.
Nuclear stain: Hoechst 33342.
Expected Localization: Cytoplasmic.
Image: A) Alpha Tubulin, B) Nuclear Stain, C) Merge, D) Secondary Only Control.

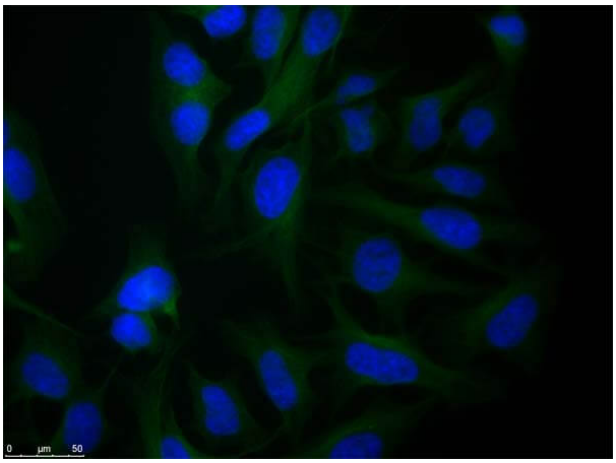

Immunofluorescence Microscopy
Immunofluorescence microscopy of Rabbit Anti-alpha-Tubulin antibody using HeLa cells fixed with PFA. Anti-alpha-Tubulin Antibody was used at 1 µg/mL, O/N at 4°C. Secondary antibody: Anti-RABBIT IgG DyLight™ 488 Conjugated Preadsorbed (p/n 611-741-127) at 2 ug/ml for 1 h at RT. Localization: TUBA1B is the major constituent of microtubules in the cytoplasm. Staining: Tubulin as green fluorescent signal with DAPI (blue) nuclear counterstain.

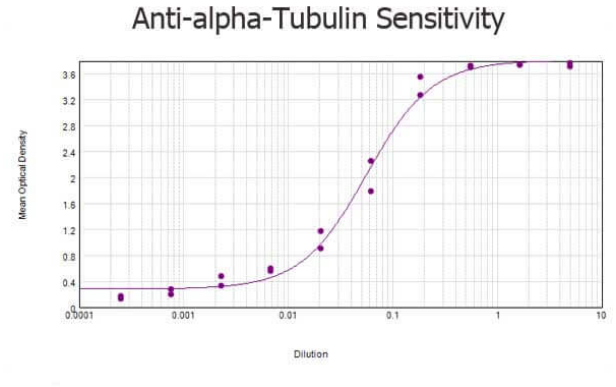

ELISA
ELISA results of purified Rabbit anti-alpha-Tubulin Antibody tested against BSA-conjugated peptide of immunizing peptide. Each well was coated in duplicate with 0.1µg of conjugate. The starting dilution of antibody was 5µg/ml and the X-axis represents the Log10 of a 3-fold dilution. This titration is a 4-parameter curve fit where the IC50 is defined as the titer of the antibody. Assay performed using 3% fish gel, Goat anti-Rabbit IgG Antibody Peroxidase Conjugated (Min X Bv Ch Gt GP Ham Hs Hu Ms Rt & Sh Serum Proteins) (p/n 611-103-122) and TMB ELISA Peroxidase Substrate (p/n TMBE-1000).

Western Blot
Western Blot of Rabbit Anti-Alpha Tubulin Antibody. Lane 1: whole cell lysates from mouse brain (p/n W10-000-T004). Lane 2: rat brain (p/n W12-000-T077). Lane 3: A431 cells (p/n W09-000-361). Lane 4: Jurkat cells (p/n W09-001-370). Lane 5: HeLa cells (p/n W09-000-364). Load: 35 µg per lane. Primary antibody: Alpha Tubulin antibody at 1:1,200 for overnight at 4°C. Secondary antibody: IRDye800™ rabbit secondary antibody at 1:10,000 for 45 min at RT. Block: 5% BLOTTO (p/n B501-0500) overnight at 4°C. Predicted/Observed size: ~50 kDa corresponding to alpha tubulin (arrowhead). Other band(s): none.

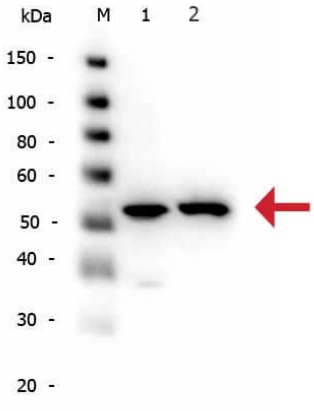

Western Blot

Western Blot of Rabbit anti-alpha-Tubulin antibody. Lane 1: HeLa WCL (p/n W09-000-364). Lane 2: NIH/3T3 WCL (p/n W10-000-358). Load: 10 µg per lane. Primary antibody: alpha-Tubulin antibody at 1:1,000 for overnight at 4°C. Secondary antibody: Peroxidase rabbit secondary antibody (p/n 611-103-122) at 1:40,000 for 30 min at RT. Block: Blocking Buffer for Fluorescent Western Blotting (p/n MB-070) for 30 min at RT. Predicted/Observed size: 50 kDa, 50 kDa for alpha-Tubulin. Other band(s): N/A.

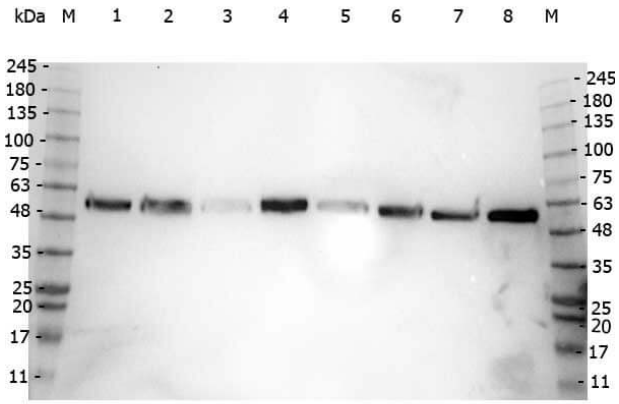

Western Blot

Western Blot of Rabbit anti-Alpha-Tubulin antibody. Marker: Opal Pre-stained ladder (p/n MB-210-0500). Lane 1: HEK293 lysate (p/n W09-000-365). Lane 2: HeLa Lysate (p/n W09-000-364). Lane 3: MCF-7 Lysate (p/n W09-000-360). Lane 4: Jurkat Lysate (p/n W09-000-370). Lane 5: A431 Lysate (p/n W09-000-361). Lane 6: LNCaP Lysate (p/n W09-001-GJ9). Lane 7: A-172 Lysate (p/n W09-001-GL5). Lane 8: NIH/3T3 Lysate (p/n W10-000-358). Load: 35 µg per lane. Primary antibody: Alpha-Tubulin antibody at 1:2,000 for overnight at 4°C. Secondary antibody: Peroxidase rabbit secondary antibody (p/n 611-103-122) at 1:30,000 for 60 min at RT. Blocking Buffer: 1% Casein-TTBS (p/n MB-082) for 30 min at RT. Predicted/Observed size: 50 kDa for Alpha-tubulin.

References

- Becker I et al. NAAG synthetase deficiency has only low influence on pathogenesis in a Canavan disease mouse model. *J Inherit Metab Dis.* (2024)
- Hardt R et al. Proteomic investigation of neural stem cell to oligodendrocyte precursor cell differentiation reveals phosphorylation-dependent Dclk1 processing. *Cell Mol Life Sci.* (2023)
- Balamurugan K et al. Stabilization of E-cadherin adhesions by COX-2/GSK3β signaling is a targetable pathway in metastatic breast cancer. *JCI Insight.* (2023)
- Polák P et al. Dual agonistic and antagonistic roles of ZC3H18 provide for co-activation of distinct nuclear RNA decay pathways. *cell Rep.* (2023)
- Garland W et al. Chromatin modifier HUSH co-operates with RNA decay factor NEXT to restrict transposable element expression. *Mol Cell.* (2022)

- Klebanovych A et al. C53 interacting with UFM1-protein ligase 1 regulates microtubule nucleation in response to ER stress. *Cells.* (2022)
- Singh J et al. Cross-linking of the endolysosomal system reveals potential flotillin structures and cargo. *Nat Commun.* (2022)
- Gerlach, P et al. Structure and regulation of the nuclear exosome targeting complex guides RNA substrates to the exosome. *Molecular Cell* (2022)
- Dillinger, AE et al. CCN2/CTGF-A Modulator of the Optic Nerve Head Astrocyte. *Frontiers in Cell and Developmental Biology* (2022)
- Wang-Eckhardt, L et al. Absence of endogenous carnosine synthesis does not increase protein carbonylation and advanced lipoxidation end products in brain, kidney or muscle. *Amino Acids* (2022)
- Grewe B et al. The HIV 5' Gag Region Displays a Specific Nucleotide Bias Regulating Viral Splicing and Infectivity. *Viruses.* (2021)
- Warner BE et al. Varicella-zoster virus early infection but not complete replication is required for the induction of chronic hypersensitivity in rat models of postherpetic neuralgia. *PLoS Pathog.* (2021)
- Wang-Eckhardt L et al. The PGRMC1 Antagonist AG-205 Inhibits Synthesis of Galactosylceramide and Sulfatide. *Cells.* (2021)
- Sheshadri N et al. PERK signaling through C/EBPδ contributes to ER stress-induced expression of immunomodulatory and tumor promoting chemokines by cancer cells. *Cell Death Dis.* (2021)
- Mietzner R et al. Angiopoietin-1 Mimetic Nanoparticles for Restoring the Function of Endothelial Cells as Potential Therapeutic for Glaucoma. *Pharmaceuticals (Basel).* (2021)
- Xiao H et al. CRNKL1 is a highly selective regulator of intron-retaining HIV-1 and cellular mRNAs. *mBio.* (2021)
- Becker I et al. Mice deficient in the NAAG synthetase II gene Rimkla are impaired in a novel object recognition task. *J Neurochem.* (2021)
- Nejedla M et al. The actin regulator profilin 1 is functionally associated with the mammalian centrosome. *Life Sci Alliance.* (2020)
- Michie J et al. Antagonism of IAPs enhances CAR T-cell efficacy. *Cancer Immunol Res.* (2019)
- Noh BJ et al. Pathogenetic implications of early growth response 1 in Ewing sarcoma. *Pathology.* (2019)
- Garland W et al. A functional link between nuclear RNA decay and transcriptional control mediated by the polycomb repressive complex 2. *Cell Rep.* (2019)
- Kim et al. Effect of HIV-1 Tat on the formation of the mitotic spindle by interaction with ribosomal protein S3. *Scientific Reports* (2018)
- Brown et al. FOXP3 and miR-155 cooperate to control the invasive potential of human breast cancer cells by down regulating ZEB2 independently of ZEB1. *Oncotarget* (2018)
- Lloret-Llinares et al. The RNA exosome contributes to gene expression regulation during stem cell differentiation. *Nucleic Acids Research* (2018)
- Ghosh et al. Little Cigars are More Toxic than Cigarettes and Uniquely Change the Airway Gene and Protein Expression. *Scientific Reports* (2017)

- Kapadia et al. Effects of sustained i.c.v. infusion of lupus CSF and autoantibodies on behavioral phenotype and neuronal calcium signaling. *Acta Neuropathologica Communications* (2017)
- Dilworth D et al. The basic tilted helix bundle domain of the prolyl isomerase FKBP25 is a novel double-stranded RNA binding module. *Nucleic Acids Res.* (2017)
- Lloret-Llinares et al. Relationships between PROMPT and gene expression. *RNA Biology* (2016)
- Liao et al. Melanopsin-expressing ganglion cells on macaque and human retinas form two morphologically distinct populations. *The Journal of Comparative Neurology* (2016)
- Li et al. Nicotinamide ameliorates palmitate-induced ER stress in hepatocytes via cAMP/PKA/CREB pathway-dependent Sirt1 upregulation. *Biochimica et Biophysica Acta* (2015)
- Besche H et al. Autoubiquitination of the 26S proteasome on Rpn13 regulates breakdown of ubiquitin conjugates. *EMBO J.* (2014)
- Gudavicius G et al. The prolyl isomerase, FKBP25, interacts with RNA-engaged nucleolin and the pre-60S ribosomal subunit. *RNA.* (2014)
- Balamurugan K et al. FBXW7α attenuates inflammatory signalling by downregulating C/EBPδ and its target gene Tlr4. *Nat Commun.* (2013)
- Hawkins ED et al. Regulation of asymmetric cell division and polarity by Scribble is not required for humoral immunity. *Nat Commun.* (2013)
- Jakobsen KR et al. Direct RNA sequencing mediated identification of mRNA localized in protrusions of human MDA-MB-231 metastatic breast cancer cells. *J Mol Signal.* (2013)
- Sarkar TR et al. Identification of a Src tyrosine kinase/SIAH2 E3 ubiquitin ligase pathway that regulates C/EBPδ expression and contributes to transformation of breast tumor cells. *Mol Cell Biol.* (2012)
- Grewe B et al. Cytoplasmic utilization of human immunodeficiency virus type 1 genomic RNA is not dependent on a nuclear interaction with gag. *J Virol.* (2012)

Disclaimer